Supporting Information for

Fabrication of Fe_7S_8/C flexible nanofibers with nano-buffered space and their application in Lithium-ion Batteries

Qianhui Wu[a], Renhua Xu[a], Chen Qian[b], Guowang Diao[a], Ming Chen[a,c*]

[a] *School of Chemistry and Chemical Engineering, Yangzhou University, Yangzhou 225002, P. R. China*

[b] *College of Chemistry and Chemical Engineering, Yangzhou Polytechnic Institute, Yangzhou 225127, P. R. China*

[c] *Key Laboratory of Advanced Energy Materials Chemistry (Ministry of Education), College of Chemistry, Nankai University, Tianjin 300071, P. R. China*

Experimental Section

Materials

All reagents are analytical grade and were directly used without any purification. Iron (III) chloride hexahydrate ($FeCl_3 \cdot 6H_2O$, AR), sodium hydroxide (NaOH, AR), sublimed sulfur, and N, N-dimethyformatide (DMF) were supplied by Shanghai Chemical Corp. Polyacrylonitrile (PAN, M_w=150000) was purchased from Aladdin. The electrolyte solution with 1M $LiPF_6$/ethylene carbonate (EC)/diethyl carbonate (DMC)/ethyl methyl carbonate (EMC) (1: 1: 1 by volume) was supplied by Guangzhou Tinci Materials Technology Co. Ltd. Other chemicals and solvents are reagent grade and commercially available. Deionized water was used for all experiments.

Characterization

* Corresponding authors.
E-mail address: chenming@yzu.edu.cn (M. Chen)

The morphologies of the samples were characterized using scanning electron microscope (SEM, Zeiss Supra 55) and Transmission Electron Microscopy (TEM, Philips Tecnai-12). High-resolution TEM (HRTEM) and high-angle annular dark-field scanning transmission electron microscopy (HAADF-STEM) were carried out on FEI Tecnai G2 F30 STWIN (USA) operating at 200 kV. X-ray diffraction (XRD) of the samples was conducted using D8 advance superspeed powder diffractometer (Bruker). Raman spectra were recorded by Renishaw in Via Raman microscope. X-ray photoelectron spectroscopic (XPS) measurements were made on Thermo Escalab 250 system. The energy-dispersive X-ray (EDX) analysis was performed on KEVEX X-ray energy detector. The magnetic measurement was characterized using vibrating sample magnetometer (VSM) (EV7, ADE, USA). Thermogravimetry analysis (TGA) (Pyris 1 TGA, PerkinElmer, USA) was performed under air atmosphere from room temperature to 800°C at a heating rate of 10°C min^{-1}. N_2 adsorption/desorption isotherm with BET and Barrett-Joyner-Halenda (BJH) analysis (Autosorb IQ3, Quantachrome Instruments, USA) were performed to clarify the specific surface area, porosity, and pore volume of the developed catalyst.

Electrochemical Tests

Lithium storage performance test were characterized using 2032 type coin cells. The half cell consists of the test anode, lithium foil as cathode, 1 M LiPF6 dissolved in a mixture of EC/DMC/EMC (1:1:1 by volume) as electrolyte, and the Celgard 2400 polypropylene as separator. All of them are assembled in a high-purity argon-filled glovebox (Vacuum Atmospheres Co., Ltd). The test anode was prepared by directly punching Fe_7S_8/C composite nanofibers film into circular electrode slice with size Φ 16 mm. Cyclic voltammetry (CV) measurements were performed on an electrochemical workstation (CHI660 E, Chenghua, CHN)

at a scan rate of 0.1 mV s^{-1} between 0.01 and 3.0 V. Electrochemical impedance spectroscopic (EIS) were carried out on an Autolab Electrochemical Analyzer (Ecochemie, Netherlands). The charge and discharge performances were recorded by a battery test system (CT-3008W, Xinwei, CHN) within a range of 0.01-3 V at different current densities.

Preparation of Fe_7S_8/C composite nanofibers

The rod-shaped α-FeOOH was prepared by a simple hydrothermal method according to reference with some modifications. About 0.75 g of polyacrylonitrile (PAN, M_W=150000) was dissolved in 10 mL of N, N-dimethylformamide (DMF) with strong magnetic stirring for 6 h. Then 0.3 g rod-shaped α-FeOOH nanoparticles were added into the DMF solution of PAN. The above-mentioned mixture solution was stirred for 10 h under room temperature. The obtained spinning solution was loaded into the syringe with a 19-gauge needle tip. For the electrospinning, the flow rate of the solution was 0.1 mL h^{-1}, the voltage between the tip and the collector was 15 kV and the distance between the tip and the collector was 15 cm. After electrospinning process, the as-prepared PAN/α-FeOOH nanofibers were stabilized at T_1 (250 ^oC) for 2 h in air. Afterwards, the nanofibers and sulfur powder were heated at T_2 (500, 600 or 700 ^oC) for 8 h under Ar atmosphere with a heating rate of 5 ^oC min^{-1}. Finally, the Fe_7S_8/C composite nanofibers were obtained by above all process. For ease of presentation, the above products are shown in Table S1.

Table S1 Abbreviation of various products with different preparation conditions.

Sample	T_1/℃	T_2/℃	Mass ratio of nanofibers to

Fe_7S_8/CNF2-500	250	500	1:2
Fe_7S_8/CNF2-600	250	600	1:2
Fe_7S_8/CNF2-700	250	700	1:2
Fe_7S_8/CNF1-700	250	700	1:1
Fe_7S_8/CNF3-700	250	700	1:3

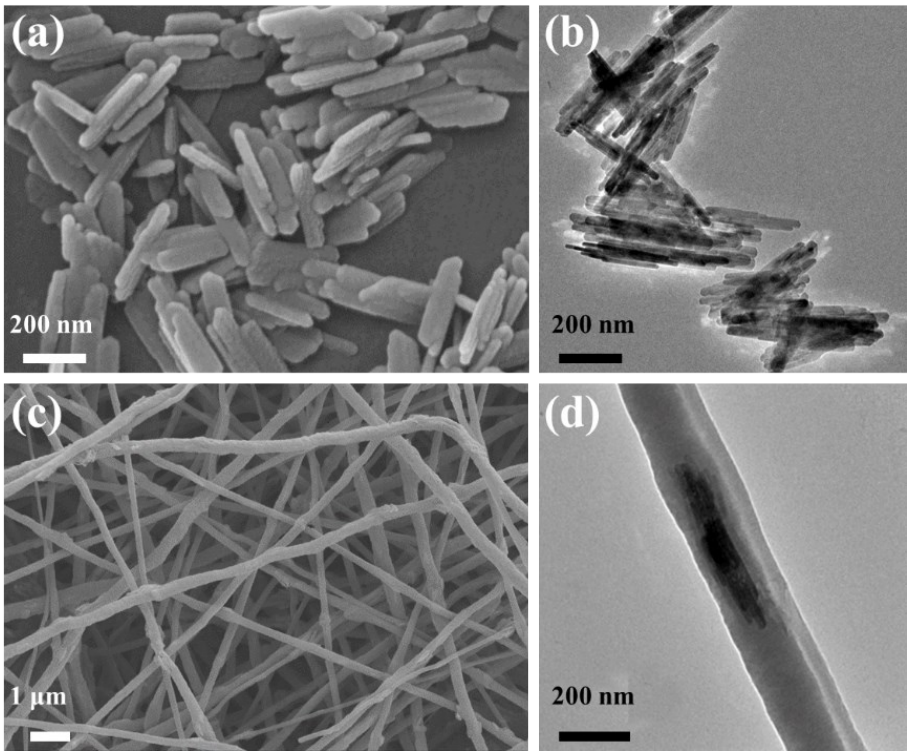

Fig. S1 SEM and TEM images of (a-b) α-FeOOH, (c-d) α-FeOOH/PAN.

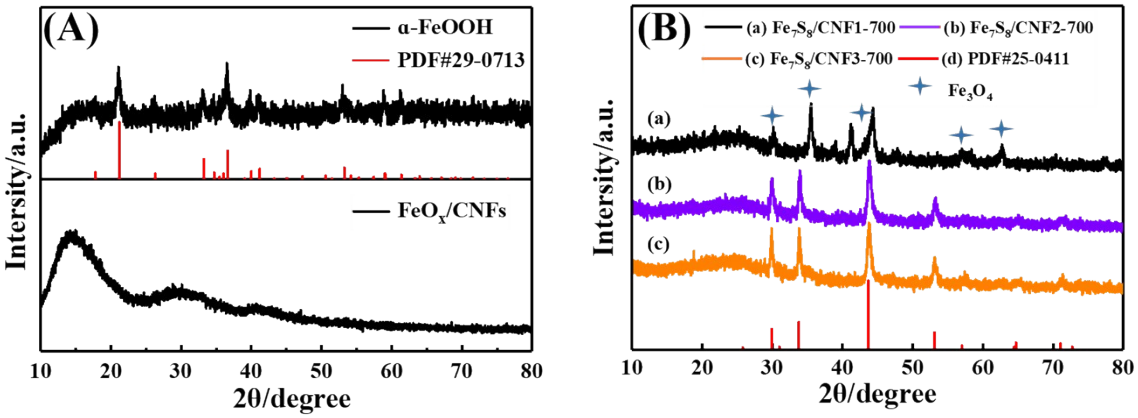

Fig.S2 (A) XRD patterns of α-FeOOH and Fe_2O_3/CNFs, (B) XRD patterns of (a) Fe_7S_8/CNF1-700, (b) Fe_7S_8/CNF2-700 and (c) Fe_7S_8/CNF3-700.

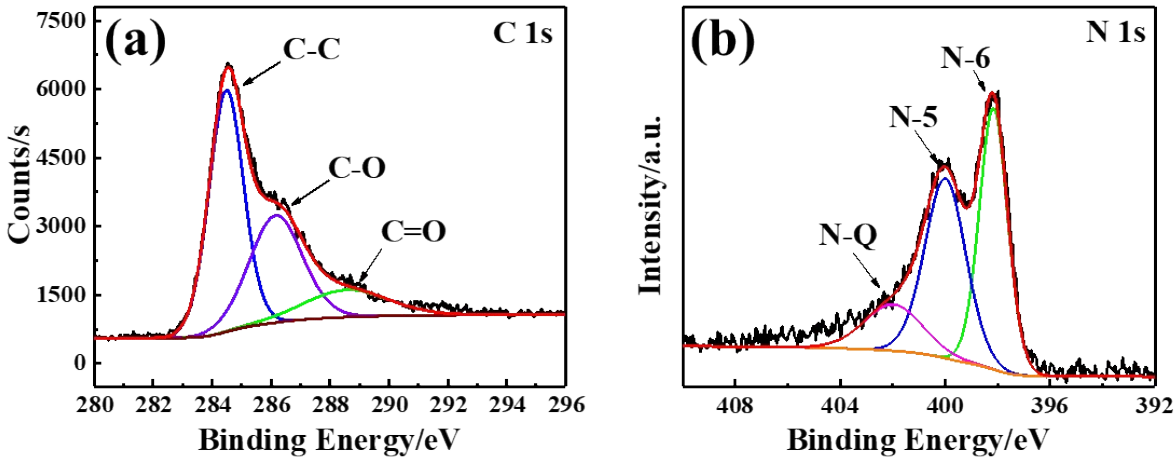

Fig. S3 XPS spectra of the Fe_7S_8/CNF2-700: high-resolution XPS spectra of (a) C1s and (b) N1s.

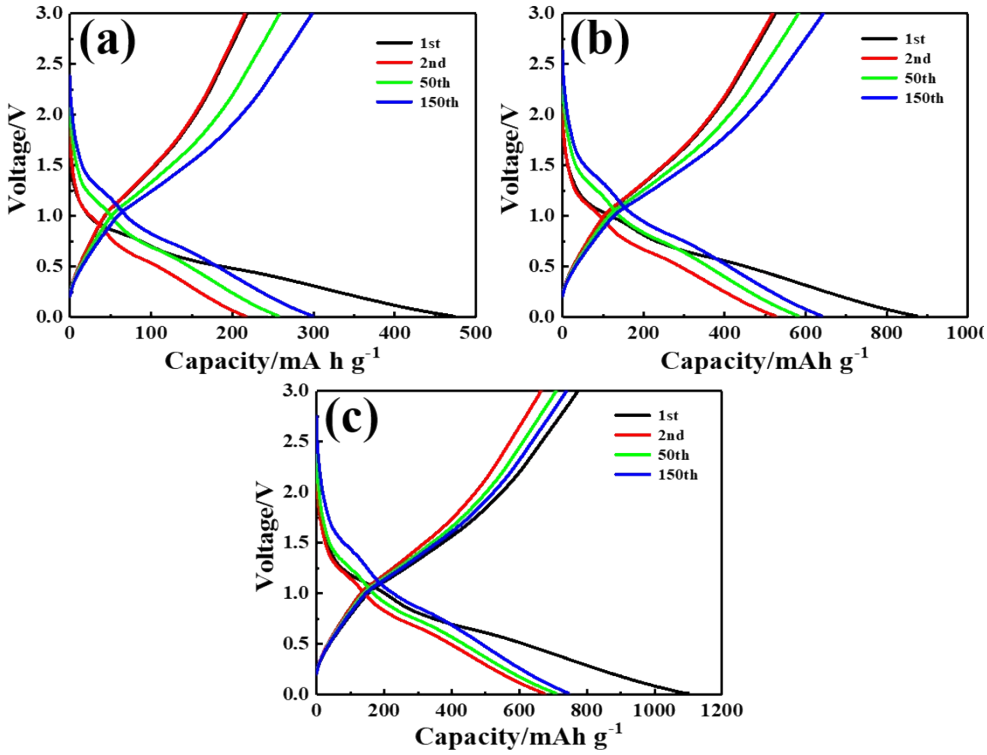

Fig. S4 Charge/discharge voltage profiles of (a) Fe_7S_8/CNF2-500, (b) Fe_7S_8/CNF2-600 and (c) Fe_7S_8/CNF2-700 at 1A g^{-1}.

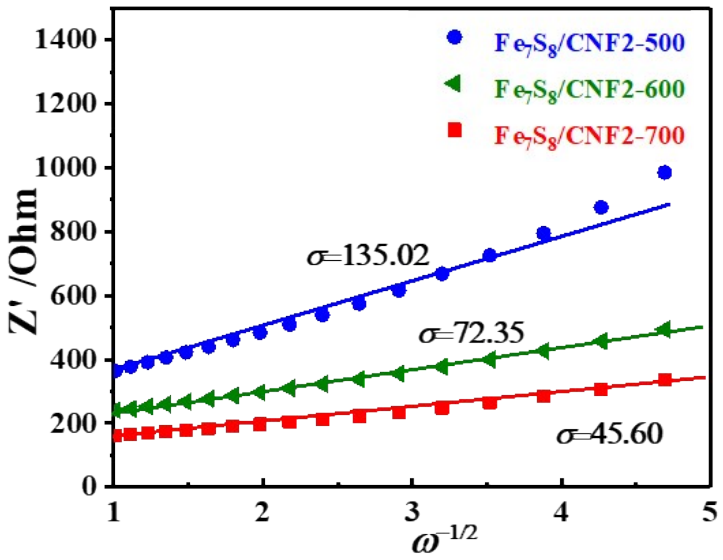

Fig. S5 Graph of the Z′ plotted against ω-1/2 at low frequency region of Fe7S8/CNF2-500，Fe7S8/CNF2-600 and Fe7S8/CNF2-700.

Table S2 Comparison between the electrochemical data of Fe_7S_8/C for LIBs performance.

Active material	Specific current	Initial capacity	nth cycle Reversible	References
Fe_7S_8@NC-PS	500	1346	1130 (100^{th})	[1]
Fe_7S_8/C/RGO	200	842	615 (500^{th})	[2]
Fe_7S_8@C (Core-shell structure)	200	1368	815 (50^{th})	[3]
Fe_7S_8@C nanorods	100	1045	825 (100^{th})	[4]
Fe_7S_8@C nanobiscuits	1000	1080	781 (500^{th})	[5]
Fe_7S_8@C nanospheres	100	442	397 (200^{th})	[6]
Fe_7S_8@C composite	2000	904	667 (200^{th})	[7]
Fe_7S_8/CNF2-700	1000	1091	675 (400^{th})	This work

Reference:

[1] Z. M. Liu, F. Hu, J. Xiang, C. Yue, D.S. Lee, T. Song, Part. Part. Syst. Char., 2018, **35**, 1800163.

[2] Y. J. Zhang, W. Chang, J. Qu, S.M. Hao, Q.Y. Ji, Z. G. Jiang, Z. Z. Yu, Chem. Eur. J., 2018, **24**, 17339.

[3] B. Y. Liu, F. H. Zhang, Q. L. Wu, J. H. Wang, W. G. Li, L. H. Dong, Y. S. Yin, Mater. Chem. Phys., 2015, **151**, 60.

[4] Q. B. Zhang, J. Liao, M. Liao, J. Y. Dai, H. L. Ge, T. Duan, W.T. Yao, Appl. Surf. Sci., 2019, **473**, 799.

[5] L. D. Shi, D. Z. Li, J. L. Yu, H. C. Liu, Y. Zhao, H. L. Xin, Y. M. Lin, C.D. Lin, C. H. Lia, C. L. Zhu, J. Mater. Chem. A, 2018, **6**, 7967.

[6] K. L. Zhang, T. L. Zhang, J. W. Liang, Y. C. Zhu, N. Lin, Y. T. Qian, RSC Adv. 2015, **5**, 14828

[7] F. Y. Jiang, Q. Wang, R. Du, X. S. Yan, Y. L. Zhou, Chem. Phys. Lett., 2018, **706**, 273.